Electrostatic correlation force of discretely charged membranes

O. González-Amezcua,[1] M. Hernández-Contreras,[1] and P. Pincus[2]
[1]*Departamento de Física, Centro de Investigación y Estudios Avanzados del Instituto Politécnico Nacional, Apartado Postal 14-740, México Distrito Federal, Mexico*
[2]*Materials Research Laboratory, University of California, Santa Barbara, California 93106*
(Received 19 April 2001; revised manuscript received 18 June 2001; published 21 September 2001)

The total force between two like charged surfaces is investigated as a function of counterion concentration in aqueous solution and surfaces distance of separation. A smooth and a discrete density of surface charge σ_s lead to differences in the force distance curve at high σ_s, which are negligible for low surface charge. The total force per unit area with divalent counterions is an oscillating function of σ_s. At fixed surfaces separation and region of attraction (increasing σ_s), there is a variation in its strength that results from a competition between the ideal kinetic and ion-ion correlation force components as predicted from the anisotropic hypernetted chain approximation.

DOI: 10.1103/PhysRevE.64.041603 PACS number(s): 68.15.+e, 82.65.+r, 68.43.−h

I. INTRODUCTION

Attractive forces between like charged objects due to the correlated fluctuations of their counterion concentration plays an important role in the adhesion of biological cell membranes [1–4]. They have been also recognized as an important mechanism for DNA to get tightly packed in a bacterial capsid, and in eukaryotic cells [5]. Experimentally these forces have been studied systematically with osmotic stress techniques in bulk aqueous solution of DNA [5], and with the use of high resolution x-ray scattering techniques in an overall neutral stack of synthetic charged membranes made of a mixture of the surfactant sodium dodecyl sulfate and the pentanol cosurfactant, in equilibrium with their dissociated counterions [6,7]. Recently, it was demonstrated that these forces arise from the correlated fluctuations of multivalent counterions that form almost two-dimensional clouds closely bound to their compensating planar charged surfaces [8]. Also condensed monovalent counterions on highly charged surfaces with a smooth distribution of charge lead to this attraction, as shown through numerical calculations of integral equation theory [9–12] and computer simulations [13–15]. Using a Gaussian fluctuation theory the asymptotic analytic expressions for this force at all separation regimes that correspond to a few angstroms were found in a model of a pair of neutral membranes formed by an equimolar mixture of a simple salt, which corresponds to the case of strongly adsorbed counterions on discretely charged surfaces [16,17]. It has been also used for counterions delocalized from the surfaces through an approximate mean field distribution [18]. In many real situations counterions are delocalized from the surfaces and distributed quite inhomogeneously [19]; therefore, the correlated pressure is very sensitive to the actual ionic profile distribution and, it is expected the pressure curve to show a more complex behavior as a function of separation, presenting, however, the asymptotic force laws cited above. We performed numerical calculations of the hypernetted chain theory (HNC) on the restricted primitive model (RPM) for continuous and discretely charged membranes with their delocalized monovalent and divalent counterions in solution, in order to determine the total pressure between pairs of membranes under different thermodynamic conditions of charge and separation. Our calculations show that independent of the way the surface charges are distributed, the pressure curves with a low to moderate surface charge σ_s coincide quantitatively, but there appears quantitative differences at very high charge density. The total pressure of monovalent counterions is repulsive in the range of charge considered. For divalent ions it is found to be repulsive for low σ_s, and attractive for high values of surface charge with its strength varying nonmonotically as a function of the surface charge. These oscillations in the pressure curve derive from the competition between the ideal kinetic and ion-ion correlations pressure contributions. Counterion profiles at low σ_s are found to be different for discrete, and smooth σ_s. However, these differences dissapear at moderate and high charge in which case the ions deplete from the middle of the slit forming a cloud closer to the surfaces. It is also noticeable that radial distribution functions of counterions that are located in the same layer, parallel, and just next to the surfaces display an accumulation of counterion pairs driven by the positional correlations with the oppositely charged neighbors.

II. MODEL SYSTEM

Two models of charged flat membranes are studied. The aqueous solvent is treated as a continuous dielectric, $\epsilon = 78.5$. Smooth and discrete distribution (of charged spheres on surfaces) are considered, neutralized by monovalent and divalent counterions that have identical size diameter $\sigma = 4.25$ Å. We shall not treat the case with added salt. Two such surfaces are separated by a mean distance h, Fig. 1. In this RPM model, N particles interact with the pairwise Coulomb potentials

$$v_i(r_{3D}) = \begin{cases} \dfrac{q_i}{\epsilon r_{3D}}, & r_{3D} > \sigma \\ \infty, & r_{3D} < \sigma, \end{cases} \tag{1}$$

where $q_i = eZ_i$ is the total charge on particle i of valence Z_i, and e is the elementary electric charge. r_{3D} is the center to center distance of separation of two particles. Each of these model membrane systems satisfy the electroneutrality condi-

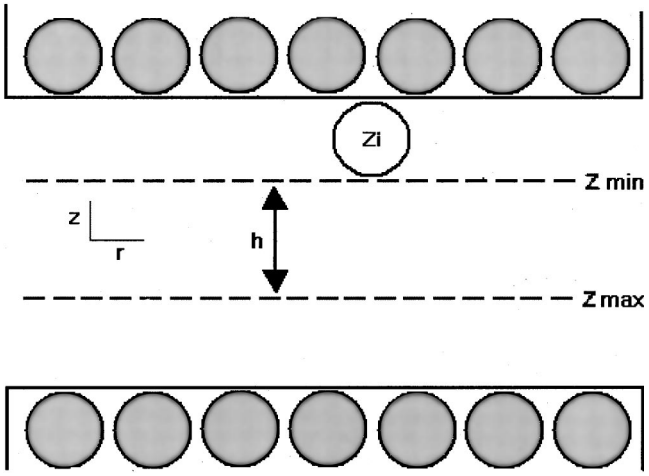

FIG. 1. A pair of like charged flat membranes separated by water $\epsilon=78.5$ a mean distance h, having each one the surface charge density σ_s. Both the counterions of valence Zi and the discrete charge on surfaces have diameter $\sigma=4.25$ Å.

tion $q\int dz\rho(z)=-2\sigma_s$, where $\rho(z)$ is the volume profile distribution of counterions in the normal direction to the planes, and σ_s the density of surface charge. We study the pressure P on the surfaces, and the equilibrium distribution of counterions with the use of the anisotropic HNC theory [10]. In this theoretical scheme the counterion distribution is determined from

$$\rho_i(z_1)=\frac{e^{\beta\mu_i}}{\Lambda_i^3}\exp\Bigg[-\beta q_i\psi(z_1)-\Sigma_j\int d\mathbf{r}dz_2\rho_j(z_2)\times\left(\frac{1}{2}h_{ij}^2(r,z_1,z_2)-c_{ij}(r,z_1,z_2)-\beta v_i(r,z_1,z_2)q_j\right)+\frac{1}{2}[h_{ij}(0,z_1,z_1)-c_{ij}(0,z_1,z_1)]\Bigg], \tag{2}$$

where Λ_i is the thermal wave length, μ_i is the chemical potential of the counterions between the surfaces that at thermal equilibrium is a constant independent of i. In the above equation

$$q_i\psi(z_1)=-2\pi\frac{q_i}{\epsilon}\sigma_s(h+\sigma)-2\pi\frac{q_i}{\epsilon}\Sigma_j\times\int dz_2|z_1-z_2|\rho_j(z_2)q_j, \tag{3}$$

where $\psi(z_1)$ is the average electrostatic potential in the counterion phase, and h the surface to surface distance of separation. The total correlation function $h_{ij}=g_{ij}-1$ and the direct correlation function c_{ij} are determined from the Ornstein-Zernike equation

$$h_{ij}(r,z_1,z_2)=c_{ij}(r,z_1,z_2)+\Sigma_\gamma\int d\mathbf{r}dz_3c_{i\gamma}(r,z_1,z_3)\times\rho_\gamma(z_3)h_{\gamma j}(r,z_3,z_2), \tag{4}$$

where r is the radial distance of separation between a pair of ions in the same ionic layer and z_i the midpoint perperdicular coordinate of layer i. This integral equation is solved with the HNC approximation

$$g_{ij}(r,z_1,z_2)=\exp[h_{ij}(r,z_1,z_2)-c_{ij}(r,z_1,z_2)-\beta v_i(r_{3D})q_j], \tag{5}$$

where $r_{3D}=\sqrt{r^2+(z_1-z_2)^2}$, and $\beta=1/k_BT$, k_B the Boltzmann's constant and $T=298$ K the temperature. In order to solve Eq. (4), the nonlinear Poisson-Boltzmann distribution obtained from Eq. (2) when the correlation functions are ignored is used as initial profile. Thereafter, new h_{ij} and c_{ij} are determined with Eqs. (4) and (5), and used as inputs for correcting the new profile given by Eq. (2) until successive iterations give updated correlation functions within 0.001% diference from the previous solutions. Up to 41 layers were used in the normal direction z to the surfaces, with 150 discrete points in the lateral direction r in a layer. Cuts of the long range tails of all correlation functions due to the Coulomb interactions were performed as described in Ref. [20]. Converging solutions were obtained after four steps of this iteration scheme. The net interaction pressure P per unit area between the surfaces is determined from

$$P=P_{kin}+P_{el}+P_{core}, \tag{6}$$

where

$$P_{kin}=k_BT\Sigma_i\rho_i(h/2), \tag{7}$$

$$P_{el}=\Sigma_{i,j}\int_0^{h/2}dz_1\rho_i(z_1)\int_{-h/2}^{0}dz_2\rho_j(z_2)\times\int d\mathbf{r}\frac{\partial\beta u_{ij}(r,z_1,z_2)}{\partial z_1}h_{ij}(r,z_1,z_2), \tag{8}$$

$$P_{core}=k_BT2\pi\Sigma_{i,j}\int_0^{h/2}dz_1\int_{-h/2}^{0}dz_2(z_1-z_2)\rho_i(z_1)\times\rho_j(z_2)g_{ij}\{[\sigma^2-(z_1-z_2)^2]^{1/2},z_1,z_2\}, \tag{9}$$

where $u_{ij}=q_iq_j/\epsilon r_{3D}$, and $\rho(h/2)$ is the density at the midpoint between the walls, P_{kin} is the ideal kinetic part, P_{el} the electrostatic correlation pressure, and P_{core} the core-core particle interaction pressure due to collisions of the ions.

III. RESULTS AND DISCUSSION

In this work we are interested in studying structural thermodynamic properties in models of pairs of charged membranes separated a mean distance h, made of a two-dimensional ionic liquid of discrete spherical negative charges of diameter σ. We will compare the same properties for the cases of a smooth density of surface charge, and that of a discrete charge distribution. A number of thermodynamic properties such as the pressure, free energy, internal energy, and counterion distribution depend on the precise knowledge of the radial distribution functions $g(r,z_1,z_2)$ of counterions in the gap between surfaces. We determined

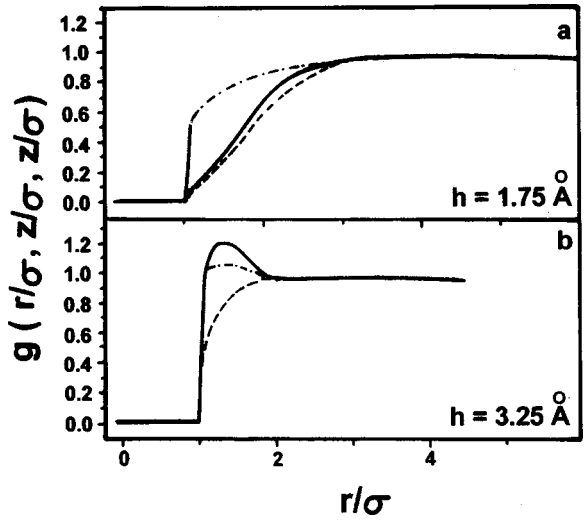

FIG. 2. In (a) are the pair correlation functions CDiv (dashed) and DDiv (dot-dashed) of divalent counterions at the ionic layer $z_1/\sigma=0.5$, with a continuous and discrete density of charge $\sigma_s=-e/285.6$ Å^2, respectively, and surface to surface separation $h=1.75$ Å. The continuous curve DDiv is the pair correlation function at midpoint between the surfaces $z_{20}/\sigma=1.4$. In (b) the same correlation functions are depicted as in (a) for the charge density $\sigma_s=-e/60$ Å^2 and $h=3.25$ Å.

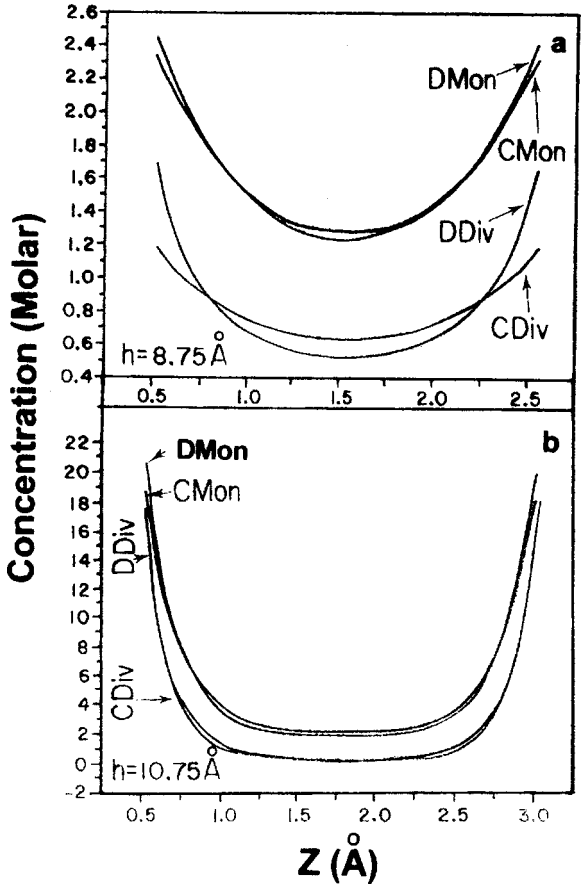

FIG. 3. Concentration profiles $\rho(z)$ of counterions of valence Zi with a continuous (CMon, CDiv) and discrete (DMon, DDiv) surface charge σ_s. (a) for $\sigma_s=-e/285.6$ Å^2 and surface- surface seperation $h=8.75$ Å; (b) for $\sigma_s=-e/60$ Å^2 and $h=10.75$ Å.

these structural properties for four systems: with a continuous (C), and discrete (D) density of surface charge σ_s, with monovalent (Mon) and divalent (Div) counterions, systems that are denoted respectively as CMon, CDiv, DMon, and DDiv. Three sets of parameter values were considered, a low $\sigma_s=-0.06675$ C/m$^2=-e/285.6$ Å^2, moderate $\sigma_s=-0.267$ C/m$^2=-e/60$ Å^2, and high $\sigma_s=-0.4$ C/m$^2=-e/40.05$ Å^2.

We consider first the lower charge density case. In Fig. 2 we plotted $g(r/\sigma,z_1/\sigma,z_2/\sigma)$ for the closest counterion layer to the wall, and for the ionic layer at the middle of the slit and two values of the surface to surface distance h. In Fig. 2(a), curve CDiv (dashed curve) is the pair correlation function of divalent counterions in the layer at the closest distance $z_1=0.5\sigma$ to the surfaces. This probability function reflects the fact that for a given σ_s continuous, an ion in layer z_1 at the origin $(r/\sigma=0)$ will find a second ion, in the same layer, and located a distance r'/σ apart, with a probability value that is lower than 1 (curve CDiv dashed). When σ_s is discrete, the presence of negative discrete charges on membranes increases this probability (dot-dashed curve DDiv) in the interval $0<r'/\sigma<3$. Therefore, electrostatic correlations among positive counterions and those negative in-plane surface charges are strongest and indirectly favors counterions to approach each other even more than when σ_s is continuous. Discretization of in-plane charge lead to correlations of ions that are less important for ions at the center of the slit, z_{20}/σ, as can be seen in Fig. 2(a), continuous curve DDiv, where this correlation function shows less structure. We recall that for the case of monovalent counterions both curves CMon and DMon do not show much differences among them at this value of σ_s.

An increase in the density of the surface charge to a moderate value $\sigma_s=-0.267$ C/m^2 and small separation $h=3.25$ Å between surfaces produces oscillations in the radial distribution functions. These are seen in Fig. 2(b) for curves DDiv and CDiv of $g(r/\sigma,z_1/\sigma,z_2/\sigma)$, which is the pair correlation function of positively charged divalent counterions. Here, as in the previous case of low charge σ_s, the discretization of surface charge led to a distribution function DDiv in layer $z_1/\sigma=0.5$ (dot-dashed curve) higher than when the surface charge is continuous (CDiv dashed), due to the stronger electrostatic correlations among counterions and surface charges. Thus, the effect of the discretization of surface charge and their correlations with ions in the bulk is to indirectly enhance the counterions accumulation in layers very close to the walls. Nonetheless, the radial distribution function of ions at the midpoint of the slit, $z_{20}/\sigma=1.4$ [Fig. 2(b), DDiv continuous curve], is even higher than for ions located at z_1/σ. Thus, for surfaces separations $h\ll 3.25$ Å, ions located in a layer at the midpoint in the slit display a more structured pattern than do those ions residing in layers closer to the surfaces at this density of charge. However, a reverse structural effect to the one discussed just above is found when the surfaces separation is increased to the intermediate value $h=10.75$ Å at this moderate charge σ_s (not depicted), where in general pair correlation functions of ionic layers closer to the walls are higher than at midway between

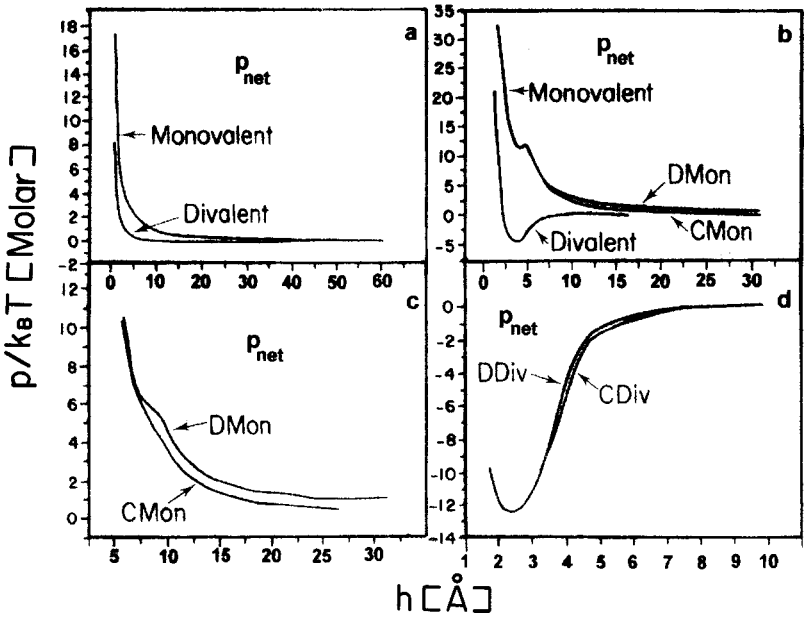

FIG. 4. The total pressure between the surfaces as a function of surfaces separation h with counterions of valence Zi; (a) for surface charge $\sigma_s=-e/285.6$ Å^2; (b) $\sigma_s=-e/60$ Å^2, (c) $\sigma_s=-e/40.05$ Å^2 for $Zi=1$ only; (d) $\sigma_s=-e/40.05$ Å^2 for $Zi=2$ only, DDiv (CDiv) curve is discrete (continuous) σ_s and divalent counterions.

walls. At the very high surface charge $\sigma_s=-0.4$ C/m^2, we find a similar behavior of all correlation functions $g(r,z_1,z_2)$ as for the case of moderate $\sigma_s=-0.267$ C/m^2 described before. We may summarize these qualitative observations as follows; for very low charge σ_s and at all separations h, the ionic layers closer to the walls are higher (more structured) than at midway distance from the surface. The same occurs in $g(r,z_1,z_2)$ for moderate and high surface charge if $h \gg 3.75$ Å. These effects on the pair correlation functions are opposite to those mentioned above when $h \ll 3.75$ Å for moderate and high σ_s, that is, $g(r,z_1,z_2)$ is more structured at the middle of the slit than for ions closer to the walls.

Once we determined the structural properties $g(r,z_1,z_2)$, we found from Eq. (2) the ionic profiles $\rho_i(z)$ in the normal direction z to the surfaces. For all the systems the separations were $h=8.75$ Å and 10.75 Å. These profiles $\rho_i(z)$ are displayed in Figs. 3(a) for $\sigma_s=-e/285.6$ Å^2, and 3(b) for $\sigma_s=-e/60$ Å^2. From these plots we observe that discretizing σ_s has the effect of depleting counterions from the middle of the slit by increasing more their concentration closer to the surfaces than in the case when σ_s is continuous. This effect is more important for divalent ions [see Fig. 3(a) for DMon and DDiv]. However, such effects due to the form of σ_s dissapears when the surfaces get separated by few ionic diameters more [Fig. 3(b)]. In general those plots show that the profile concentration associated with monovalent ions is higher than for divalent ones. This is so because more elementary monovalent charges are required to compensate the surface charges. In these plots we show the modification of the profile concentrations $\rho(z)$ as a function of surface separations and density of charge σ_s. These plots show that at larger surface separations the counterions get confined to the surfaces, condensing closer to them, and vanish their concentration at the middle of the slit for any valence of ions. Many quantitative differences are not observed in the profiles regardless of whether σ_s is discrete or continuous. A similar effect occurs if the density of surface charge is increased while h is kept fixed. At the highest value of σ_s considered we noticed $\rho(z)$ is almost the same irrespective of the structure given to the distribution of surface charge σ_s and valence Z_i. The counterions increase their concentration profile closer to the membrane surfaces as h gets larger, and develops oscillations for monovalent counterions.

Having addressed the problem of determining the profiles density $\rho_i(z)$ we calculated the total pressure from Eq. (6). At the low surface charge $\sigma_s=-0.066\,75$ C/m^2 the net counterion pressure P for both $Z_i=1$ and 2 is repulsive at all surface-surface separations h. It is also found that the strength of the core-core pressure component is higher for $Z_i=1$ than for $Z_i=2$ at all separations h and surface charge σ_s. A fact that comes about from the larger frequency of contacts among monovalent ions and also due to their higher concentration. However, the electrostatic correlation pressure component is always more important for $Z_i=2$ due to the strongest electrostatic interactions than for $Z_i=1$. For a given valency of ions the net pressure curves are quantitatively the same irrespective of whether σ_s is discrete or continuous [see Fig. 4(a)] for σ_s low.

We found above that the total pressure for low surface charge $\sigma_s=-0.066\,75$ C/m^2 was always repulsive with any valence of counterions. At the moderate value $\sigma_s=-0.267$ C/m^2 we find now that the net pressure curve of divalent ions display already an attractive region at the very short surfaces separation range 1 Å$<h<$10 Å, and turns into repulsive for large h, vanishing for $h>25$ Å in both cases of continuous (effect already observed by Kjellander *et al.*, [9]), and discrete charge. A quite different behavior is shown by the pressure curve of monovalent ions which at all separations is always repulsive with a small shoulder at about $h=5$ Å due to core-core repulsive ion interactions [see Figs. 4(b) DMon and CMon], and lowering its strength slowly at very large separation h. Therefore, for this surface charge monovalent ions induce a repulsive pressure at all separation distances and remains non-negative. Even at this surface charge ($\sigma_s=-0.267$ C/m^2) and any valence Z_i of ions there is no quantitative differences in the net pressure

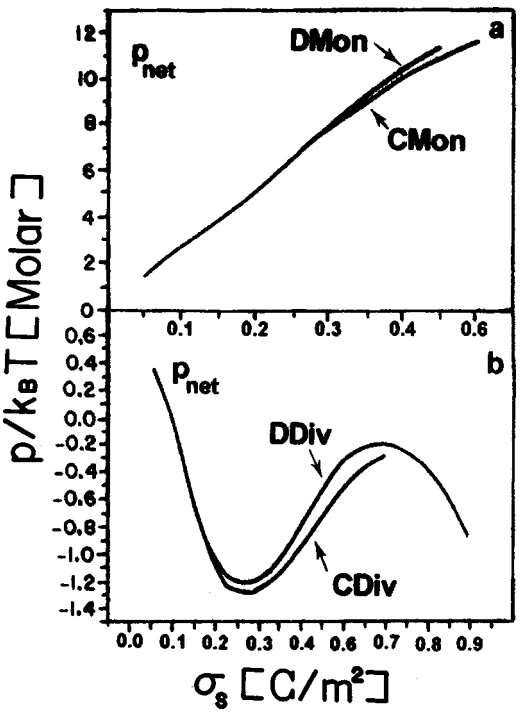

FIG. 5. (a) The pressure curve of monovalent counterions as a function of the density of surface charge σ_s and fixed surface-surface separation $h=5.75$ Å. (b) The pressure of divalent counterions as a function of σ_s for $h=5.75$ Å. The other symbols are as in Fig. 4.

and its components when σ_s is continuous or discrete. The most important effect of increasing the surface charge on the thermodynamic properties appears in the net pressure between membranes as will be made clear below. Only at high surface charge the effect of discretizing σ_s becomes relevant and leads to quantitative differences in net P at all separations h, see Figs. 4(c) and 4(d) for monovalent and divalent counterions, respectively. The net pressure associated to divalent ions turns always to a negative value for all h [Fig. 4(d)]. Finally, Figs. 5(a) and 5(b) give us the dependence of the net pressure P on the density of charge σ_s for $Z=1,2$ and $h=5.75$ Å, respectively. Here again net P of $Z=1$ and 2 shows differences at higher σ_s. The net pressure of divalent counterions display oscillations as a function of σ_s, meanwhile P of monovalent ions is always an increasing function of σ_s and is repulsive.

IV. CONCLUSION

In this work we reported that discretization of the surface charge on two equally and highly charged surfaces separated a mean distance by a counterion solution can lead to differences on the pressure curve as a function of surfaces separation for any valence of counterions, as compared with the pressure for surfaces with a smooth distribution of charge. These quantitative differences disappear at low σ_s. The pressure curve of divalent counterions is repulsive at very low σ_s and turns into attractive at high charge density. In this attractive range the strength of the total pressure varies with increasing σ_s due to a partial compensation of the ion-ion correlation pressure that outweighs the ideal kinetic contribution to the total pressure, components that, however, change their relative strengths with σ_s. Unlike the divalent case, the net pressure curve with monovalent counterions is always repulsive for any charge considered.

ACKNOWLEDGMENTS

This work was supported by a Conacyt Grant No. 32169-E, México. P.P. acknowledges support by the MRL program of the National Science Foundation under Award No. DMR96-32716.

[1] V.A. Parsegian, R.P. Rand, and D.C. Rau, in *Physics of Complex and Supermolecular Fluids*, edited by S.A. Safran and N.A. Clark (Wiley, New York, 1987).
[2] J. Israelachvili, *Intermolecular and Surface Forces* (Academic Press, New York, 1992).
[3] V.A. Parsegian and D. Gingell, Biophys. J. **12**, 1192 (1972).
[4] J. Nardi, T. Feder, R. Bruinsma, and E. Sackmann, Europhys. Lett. **37**, 371 (1997).
[5] V.A. Bloomfield, Curr. Opin. Struct. Biol. **96**, 334 (1996).
[6] D. Roux and C.R. Safinya, J. Phys. (Paris) **49**, 307 (1988).
[7] R.M. Servuss and W. Helfrich, J. Phys. (Paris) **50**, 809 (1989).
[8] I. Rouzina and V.A. Bloomfield, J. Phys. Chem. **100**, 9977 (1996).
[9] R. Kjellander, T. Åkesson, B. Jönsson, and S. Marcelja, J. Chem. Phys. **97**, 1424 (1992).
[10] R. Kjellander and S. Marcelja, Chem. Phys. Lett. **127**, 402 (1986).
[11] M. Hernández-Contreras and P. Pincus, J. Chem. Phys. **112**, 954 (2000).
[12] P.H. Attard, R. Kjellander, and D.J. Mitchell, J. Chem. Phys. **89**, 1664 (1988).
[13] L. Guldbrand, B. Jönsson, H. Wennerström, and P. Linse, J. Chem. Phys. **80**, 2221 (1984).
[14] N. Grønbech-Jensen, R.J. Mashl, R. Bruinsma, and W.M. Gelbart, Phys. Rev. Lett. **79**, 2582 (1997).
[15] R.J. Mashl and N. Grønbech-Jensen, J. Chem. Phys. **109**, 4617 (1997).
[16] P.A. Pincus and S.A. Safran, Europhys. Lett. **42**, 103 (1998).
[17] R. Podgornik and B. Zeks, J. Chem. Soc., Faraday Trans. 2 **84**, 611 (1988).
[18] D.B. Lukatsky and S.A. Safran, Phys. Rev. E **60**, 5848 (1999).
[19] S.A. Safran, *Statistical Thermodynamics of Surfaces, Interfaces and Membranes* (Addison-Wesley, Reading, MA, 1994).
[20] J.P. Hansen and I.R. McDonald, *Theory of Simple Liquids* (Academic, London, 1986).